Journal of Hazardous Materials 402 (2021) 123567

Contents lists available at ScienceDirect

Journal of Hazardous Materials

journal homepage: www.elsevier.com/locate/jhazmat

The effect of cationic surfactants on improving natural clinoptilolite for the flotation of cesium

Muhammad Yusuf Prajitno [a,*], Suparit Tangparitkul [b], Huagui Zhang [c], David Harbottle [a], Timothy N. Hunter [a,*]

[a] School of Chemical and Process Engineering, University of Leeds, Leeds, LS2 9JT, UK
[b] Department of Mining and Petroleum Engineering, Chiang Mai University, Chiang Mai, 50200, Thailand
[c] College of Chemistry and Materials Science, Fujian Province Key Laboratory of Polymer Science, Fujian Normal University, Fuzhou, 350007, China

ARTICLE INFO

Editor: T. Meiping

Keywords:
Cesium
Clinoptilolite
Flotation
Ion exchange
Cationic surfactants

ABSTRACT

Flotation using cationic surfactants has been investigated as a rapid separation technique to dewater clinoptilolite ion exchange resins, for the decontamination of radioactive cesium ions (Cs^+) from nuclear waste effluent. Initial kinetic and equilibrium adsorption studies of cesium, suggested the large surface area to volume ratio of the fine zeolite contributed to fast adsorption kinetics and high capacities (q_c = 158.3 mg/g). Adsorption of ethylhexadecyldimethylammonium bromide (EHDa-Br) and cetylpyridinium chloride (CPC) surfactant collectors onto both clean and 5 ppm Cs^+ contaminated clinoptilolite was then measured, where distribution coefficients (K_d) as high as 10,000 mL/g were evident with moderate concentrations CPC. Measurements of particle sizes confirmed that adsorption of surfactant monolayers did not lead to significant aggregation of the clinoptilolite, while < 8% of the 5 ppm contaminated cesium was remobilised. Importantly for flotation, both the recovery efficiency and dewatering ratios were measured across various surfactant concentrations. Optimum conditions were found with 0.5 mM of CPC and addition of 30 μL of MIBC frother, giving a recovery of ~90% and a water reduction ratio > 4, highlighting the great viability of flotation to separate and concentrate the contaminated powder in the froth phase.

1. Introduction

Cesium-137 (^{137}Cs) is a beta-emitting radioisotope, which is obtained from the fission of uranium-235 and other isotopes in nuclear activities. It is one of the highest yield, medium-lived fission products in nuclear reactors (at around 6.3 %) with an activity of 3.215 T Bq/gr and half-life ~30 years (Nagasaki and Nakayama, 2015; Ojovan and Lee, 2014). It is also highly water soluble, and in small amounts can cause cancer, while in larger doses causes severe acute sickness or even death (Abusafa and Yücel, 2002; Nagasaki and Nakayama, 2015; Ojovan and Lee, 2014; Smičiklas et al., 2007; Zhang et al., 2017). In order to prevent the free release of this radioactive waste through the environment, the nuclear industry commonly uses clinoptilolite as an ion exchange media during effluent treatment processes (Abusafa and Yücel, 2002; Elizondo et al., 2000; Ojovan and Lee, 2014; Petrus and Warchoł, 2003; Smičiklas et al., 2007). Clinoptilolite is a naturally occurring zeolite with good selectivity for ^{137}Cs removal and excellent resistance to radiation exposure, and has attracted a large body of research into its use (e.g. (Abusafa and Yücel, 2002; Amanipour and Faghihian, 2017; Ames, 1962; Borai et al., 2009; Endo et al., 2013; Faghihian et al., 1999; Ojovan and Lee, 2014; Rajec and Domianová, 2007; Rajec et al., 1998; Smičiklas et al., 2007)). For example, within the United Kingdom, it is currently used as an ion exchange resin for cesium and strontium removal for effluents from nuclear fuel cooling ponds (Dyer, 1993; Dyer et al., 2018; Owens et al., 2015).

While there are a number of alternative techniques to remove radioisotopes from nuclear effluents; including co-precipitation and coagulation methods, membrane techniques or the combined use of powdered surface adsorbents (Abusafa and Yücel, 2002; Aziz and Beheir, 1995; Boglaienko et al., 2019; Ding et al., 2017; Dyer et al., 2018; Fu and Wang, 2011; James et al., 2019; Olatunji et al., 2015; Ortiz-Oliveros et al., 2012; Smičiklas et al., 2007; Xu et al., 2017), the use of ion exchange media is still among the most industrially common, due to the high specific decontamination factors and low production of secondary wastes (James et al., 2019; Olatunji et al., 2015; Zhang et al., 2017). There are also a number of techniques to improve the

* Corresponding authors.
E-mail addresses: pmmyp@leeds.ac.uk (M.Y. Prajitno), t.n.hunter@leeds.ac.uk (T.N. Hunter).

https://doi.org/10.1016/j.jhazmat.2020.123567
Received 25 February 2020; Received in revised form 30 April 2020; Accepted 21 July 2020
Available online 27 July 2020

performance of zeolite and clay ion exchange resins for heavy metal removal, such as milling, chemical activation and the use of synthetic modifications or composites (Amanipour and Faghihian, 2017; Borai et al., 2009; De Haro-Del Rio et al., 2015; Faghihian et al., 2015; Han et al., 2019; Li et al., 2019). For example, the production of finely milled particles can enhance the uptake of cesium, in line with increases to the specific surface area of adsorbent (Prajitno et al., 2020). Unfortunately, size reduction of ion exchange media would make such particles no longer suitable for use in elution columns, due to the increased pressure loss and related reduction in available flowrates (Abusafa and Yücel, 2002; Dyer et al., 2018).

Fine, powdered ion exchange resins may, however, be used in large batch processes, when combined with co-precipitation methods to aid separation rates (Kim et al., 2019; Rogers et al., 2012; Teh et al., 2016) such as in cesium removal (Rashad et al., 2019; Shakir et al., 2007). Unfortunately, solid-liquid dewatering rates of these types of sludges is slow, resulting in voluminous secondary wastes that are difficult to treat themselves. Therefore, to overcome these issues, flotation is investigated in this study as an alternative process to separate fine and highly efficient powdered ion exchange material, with greater dewatering factors and considerably smaller residence times than is possible from gravitational sedimentation (Deliyanni et al., 2017; Peleka et al., 2018; Rashad et al., 2019).

Flotation is commonly used in a number of applications, either for removing heavy metal ions, to separate minerals from gangue material or simply as a rapid technique to dewater suspensions, where the concentrated sludge fraction is removed along with the froth (Atkin et al., 2003; Huang et al., 2003; Mavros and Matis, 2013; Wu et al., 2019; Zhang et al., 2019b). Particle or aggregate flotation is based on the removal of solids through adsorption onto foam interfaces, by using surface active agents (surfactants) as collectors to modify particle contact angles (Atkin et al., 2003; Fu and Wang, 2011; Huang et al., 2003; Hunter et al., 2008; Le et al., 2012; Ortiz-Oliveros et al., 2012; Polat and Erdogan, 2007; Wu et al., 2019; Zhang et al., 2019b). In order to achieve a successful flotation process, the selection of a suitable collector is required in order to maximize the hydrophobicity of the particles to ensure strong adsorption to bubble interfaces (Hunter et al., 2008; Polat and Erdogan, 2007; Rahman et al., 2012; Zamboulis et al., 2004; Zhang et al., 2019a). Often, a separate frother additive is also used, such as methyl isobutyl carbinol (MIBC), to obtain rapid flotation with fine bubbles (Mavros and Matis, 2013; Polat and Erdogan, 2007; Zhang et al., 2019a).

There are many industrial sectors that use flotation as an engineering solution, such as minerals processing, wastewater treatment and paper recycling, while it is a technique of increasing interest for nuclear effluent treatment (Atkin et al., 2003; De Haro-Del Rio et al., 2015; Deliyanni et al., 2017; Dhenain et al., 2009; Han et al., 2018; Hu et al., 2018; Huang et al., 2003; Karimi et al., 2008; Mahmoud et al., 2015; Mavros and Matis, 2013; Polat and Erdogan, 2007; Rahman et al., 2012; Wu et al., 2019; Zamboulis et al., 2004; Zhang et al., 2019b). In terms of its application in nuclear related fields, ion flotation and combined co-precipitation methods have been used to remove radioisotopes of cesium, strontium and cobalt, while fine particle flotation has been used for the separation of soils and as part of nuclear wastewater treatment processes (Aziz and Beheir, 1995; Charewicz et al., 2001; De Haro-Del Rio et al., 2015; Micheau et al., 2015; Ortiz-Oliveros and Flores-Espinosa, 2019; Ortiz-Oliveros et al., 2012; Shakir et al., 1993, 2007). It has also been demonstrated recently as a viable technique for the separation of cesium contaminated colloidal clays (Zhang et al., 2017, 2019a).

Given the evidence that flotation can be used as a successful technique for nuclear effluent treatment from previous research, it is perhaps surprising there has been no previous specific studies into its use to separate contaminated clinoptilolite, although previous work by Walcarius et al. (2001) into the flotation of lead-adsorbed faujasite highlights its potential in similar systems. However, there are some significant questions that remain into the potential viability of this process. Perhaps most importantly, is the potential for surfactant collectors to remobilise and remove contaminated radioisotopes that have been adsorbed, and additionally, whether the effect of ion contamination reduces the interaction of the collectors and thus flotation removal. Also, for flotation to be considered for rapid dewatering, the process needs to be optimised to not only maximise recovery, but also reduce water carry-over in the froth phase, to ensure good dewatering ratios.

Therefore, in this study, the flotation performance of cesium contaminated, fine clinoptilolite is investigated. The type of material processed, is based upon post-adsorption ion exchange powder, utilised for the removal of radioisotopes from nuclear effluents in batch contact tanks. Two cationic surfactants (Ethylhexadecyldimethylammonium bromide and Cetylpyridinium chloride) are used as collectors, where their adsorption density and structure is measured on both clean and contaminated material. The flotation recovery of the contaminated clinoptilolite is optimised by varying both collector concentration and through the addition of MIBC frother, where importantly, both flotation removal and dewatering ratio are measured.

2. Experimental

2.1. Materials

Natural clinoptilolite was supplied from Fluorochem as a nominal ±7 μm powder (product code S25114). Cesium chloride (CsCl) Analytical Grade with purity ≥ 99.0 % was purchased from Sigma-Aldrich. For surfactant adsorption and flotation studies, two cationic surfactants were selected; Ethylhexadecyldimethylammonium bromide (EHDA-Br) and Cetylpyridinium chloride (CPC) supplied by Merck Millipore and Sigma-Aldrich, respectively. EHDA-Br has previously been used for the flotation of cesium contaminated clays (Zhang et al., 2019a), while CPC is an ammonium based cationic surfactant of the same chain length with a pyridine head group, and has been used previously to float metal ions (Aziz and Beheir, 1995; Soliman et al., 2015; Walcarius et al., 2001). Methyl isobutyl carbinol (MIBC) with purity ≥ 99.0 % (Sigma-Aldrich) was used as a frother, as common in flotation studies (Mavros and Matis, 2013; Polat and Erdogan, 2007; Zhang et al., 2019a).

2.2. Particle characterisation

The zeta potential of 1 wt% clinoptilolite dispersions was measured using a Zeta Probe (Colloidal Dynamics) in order to determine the change in surface charge of natural clinoptilolite through adsorption of different concentrations of cesium salt. Fig. S1 within the Electronic Supplementary Material (ESM) shows the zeolite particle zeta potential versus initial concentration of cesium ions, where it is evident that although the potential becomes lower in magnitude with Cs^+ adsorption, it remains negative under all concentrations. This result infers cationic surfactants will interact strongly with the surface across a wide range of cesium contaminations (Prajitno et al., 2020).

To analyse the powder structure, a TM3030 (Hitachi Ltd.) bench top scanning electron microscope (SEM) was used to image the clinoptilolite powder, as shown in the ESM (Fig. S2) at two scales. The powder presents itself as irregular shaped crystals, consistent with crushed zeolite minerals from other studies (Abusafa and Yücel, 2002; Amanipour and Faghihian, 2017; Ames, 1962; Borai et al., 2009; Endo et al., 2013; Faghihian et al., 1999; Petrus and Warchoł, 2003; Prajitno et al., 2020; Rajec and Domianová, 2007; Rajec et al., 1998; Smičiklas et al., 2007). Sizing from SEMs suggested all particles were < 30 μm, in agreement with supplier specifications. The Brunauer–Emmett–Teller (BET) particle surface area was determined with a Tristar 3000 (Micrometrics) using the same procedure as outlined in previous research (Prajitno et al., 2020). The resultant surface area was measured as 44.7 m^2/g, which is consistent to that of < 53 μm milled clinoptilolite particles previously characterised by the current authors (Prajitno et al., 2020).

2.3. Cesium adsorption on clinoptilolite

To measure adsorption kinetics, cesium chloride (CsCl) stock solution (1 M) was diluted with Milli-Q water at neutral pH (which tends to a pH of ~6.5) to a nominal initial concentration of 5 ppm, in line with previous studies on cesium adsorption (Kim et al., 2017; Zhang et al., 2017). The 5 ppm solution was then filled into a polypropylene conical centrifuge tube. Polypropylene tubes were used in order to prevent Si contamination from glassware and also potential of Cs^+ adsorption onto the tubes, as evidenced in an earlier study (Chorover et al., 2003). Then, natural clinoptilolite was dispersed into the solution at a fixed 20 g/L solid/liquid ratio. All suspensions were then placed on an orbital shaker at 150 rpm (at room temperature) for different times from 30 min until 48 h. The suspensions were then centrifuged using a Heraeus Megafuge 16R (Thermo-Scientific) for 10 min at 7000 rpm, and the separated supernatants were decanted using a 20 mL syringe with 0.3 μm filter. Cesium concentrations from extracted supernatants were measured using a 240FS Atomic Absorption Spectrophotometer (AAS) (Varian-Agilent) utilising a cesium lamp set with a wavelength of 459.3 nm (suitable for concentrations from 5 to 4000 ppm).

The amount of Cs^+ adsorbed by clinoptilolite at different specific times was determined from AAS measurements, in terms of the relative kinetic adsorption amount, q_t (mg/g) and removal percent, using the methodologies described within the ESM (Eq. S.1-S.2). Adsorption kinetic fits were determined using the Pseudo Second Order (PSO) rate model to derive the adsorption rate constant (k_2) and the initial rate of adsorption (h) (see ESM, Eq. S.3 or as detailed within a previous publication by the current authors (Prajitno et al., 2020)).

For the equilibrium adsorption study, 1 M CsCl stock solution was diluted with Milli-Q water at neutral pH in order to get various initial concentrations from 5 ppm up to 4000 ppm with a solid/liquid ratio fixed at 20 g/L. All suspensions were then placed on an orbital shaker for 48 h, with supernatants being extracted and analysed by AAS as described above. Equilibrium data was fitted with both Langmuir and Freundlich isotherm monolayer adsorption models (see ESM, Eqs. S.4-S.5).

2.4. Surfactant adsorption at the air-liquid and solid-liquid surface

The two cationic surfactants were prepared in different concentrations from 0.01 mM to 20 mM. To obtain desired concentrations, 1 M of EHDA-Br and CPC solutions were diluted with Milli-Q water at neutral pH. The solutions were then analysed using a Theta Optical Tensiometer (Biolin Scientific) in order to measure the air-water surface tension via droplet profiling. The instrument was housed in a temperature-controlled chamber (20 °C +/- 0.5 °C) and a constant droplet size (~10 μL) was used for all experiments. Surface tension versus surfactant concentration data were also fitted to the Langmuir monolayer model, for concentrations below the critical micelle concentration, given in Eq. (1).

$$\gamma = \gamma_0 + RT\Gamma_{max}\ln\left(\frac{1}{1+KC}\right) \quad (1)$$

Here, γ (N/m) is the fitted surface tension for a specific surfactant initial concentration, C (M), γ_0 is the surface tension of the pure solvent, R is the universal gas constant (8.315 J/mol.K), T is system temperature (293.15 K), while Γ_{max} is the maximum surface coverage of surfactant (mol/m^2) and K is the equilibrium constant (M^{-1}) (James et al., 2018; Stanimirova et al., 2011). Model fits were obtained numerically by minimising the error between theoretical calculated values of surface tension and measured readings using MS Excel Solver™, with Γ_{max} and K the independent variable parameters. The goodness of fit was determined using the R^2 ('RSQ') function.

Surface tension tests were also used to measure the amount of cationic surfactant adsorbed onto both natural and pre-contaminated clinoptilolite (which had been initially mixed with 5 ppm of Cs^+ for 24 h before separation, washing and drying). After mixing different concentrations of both surfactants with 20 g/L clinoptilolite suspensions for 24 h, the clear supernatants were extracted and filtered to remove any particles, as described above in Section 2.3. The surface tension of these supernatant solutions was then measured and compared to the Langmuir fits of the pure surfactants to determine the concentrations after adsorption (via back-calculation), and thus importantly, the amounts adsorbed. Additionally, a control supernatant solution from surfactant-free dispersions was examined to determine the contribution of any fine nanoparticles (< 200 nm) that may possibly have been left in the supernatant solution. The measured surface tension was ~72.8 mN/m, and thus close to the expected value for pure water-air, confirming minimal influence on measured values (Binks, 2002; Hodges and Tangparitkul, 2019).

Additionally, the influence of surfactant adsorption on particle stability was assessed by measuring the particle size distribution of 5 ppm Cs-contaminated clinoptilolite (at 20 g/L) with different concentrations of both cationic surfactants (from 0.01 mM to 20 mM). The suspensions were mixed on an orbital shaker at 15 rpm (at room temperature) for 24 h, before being placed in Grant XUBA3 ultrasonic bath for 5 min in order to fully disperse. Suspensions were then analysed using a Mastersizer 2000E laser diffractometer (Malvern Panalytical Ltd).

2.5. Flotation experiments

Flotation experiments were performed by adding 3 g of dried 5 ppm Cs-contaminated clinoptilolite into a laboratory-scale flotation cell (column diameter and height: 65 mm and 97 mm) as utilised in a previous study by the authors (Zhang et al., 2019a). Foam was generated from direct injection of air through a sintered glass plate with micron-sized pores (see ESM, Fig. S3). Different concentrations of the cationic surfactants, from 0.01–20 mM, were added into the cell, with the solid/liquid ratio fixed at 20 g/L. The agitation of the suspension was provided by an overhead stirrer, with a 0.75 inch, 4-blade, 45° pitched impeller rotating at 300 rpm for 5 min. The air flowrate was fixed at 0.2 L/min. To measure the material separated in the froth, the overhead stirrer was reduced to 100 rpm for 10 min and 50 μL of MIBC frother was added to the suspension (which is a similar amount to that previously reported for the flotation of Cs-contaminated clays (Zhang et al., 2017)) while the air flowrate was increased to 0.7 L/min. The change from low to high gas flow rate was performed to increase the interfacial area and turbulence at the interface, generating effective contact of the particles in the froth (Darton and Sun, 1999). The froth containing recovered Cs^+ contaminated clinoptilolite was collected into a 400 mL beaker, before being dried at 90 °C and weighed in order to study the recovery (see ESM, Eq S.8). The volume of the remaining liquid fraction was measured, in order to calculate water reduction ratio, as given in Eq. (2), which is a critical parameter in order study the dewatering efficiency of the flotation operation (Mahmoud et al., 2017; Rashad et al., 2019; Soliman et al., 2015).

$$\text{Water reduction ratio} = \frac{V_0}{V_0 - V_e} \quad (2)$$

where V_0 (mL) is the initial volume of the suspension and V_e (mL) is the volume of liquid remaining in the flotation cell after completion.

Additionally, in order to study the effect of varying frother concentration, the same process was repeated with a fixed concentration of cationic surfactant and variable added frother volume up to 50 μL. The effect of variable cesium contamination was also studied, using clinoptilolite prepared by repeating the same procedure from 2.4, where initial cesium concentration was varied from 5 to 1000 ppm. Then, flotation extraction was repeated using a fixed concentration of CPC type surfactant and the addition of the optimal frother volume.

3. Results and discussion

3.1. Cesium adsorption onto clinoptilolite

Initial batch ion adsorption experiments were conducted to understand both the equilibrium adsorption of cesium on the clinoptilolite and its adsorption kinetics. The equilibrium adsorption data is given in Fig. 1, presented in terms of the equilibrium Cs^+ concentration, along with associated Freundlich and Langmuir monolayer fits (for details for fitting, see ESM, Fig. S4 and Table S1).

The performance of the clinoptilolite at removing cesium compares very favourably to other research on similar materials (Amanipour and Faghihian, 2017; Borai et al., 2009; De Haro-Del Rio et al., 2015; Faghihian et al., 1999; Petrus and Warchoł, 2005; Prajitno et al., 2020; Smičiklas et al., 2007). In fact, cesium adsorption capacity is about twice that of unmodified clinoptilolite sourced from a different supplier that was used by the same authors in a previous study (Prajitno et al., 2020), highlighting likely low levels of ion-contamination in the zeolite (which was shown to reduce adsorption with the other material (Prajitno et al., 2020)). Secondly, its strong performance is also likely due to its small particle size (<30 μm) giving a large surface area to volume ratio (and thus a relative increase in surface exchange sites), where it has also been shown previously by the current authors that milling low-grade clinoptilolite to smaller sizes with a similar surface area considerably increased its capacity (Prajitno et al., 2020). It is noted that as clinoptilolite is generally used as bead material in ion-exchange columns, the usable size range is much larger (with associated lower surface to volume ratio). Therefore, if flotation can be used as a viable rapid separation method for such fine particles, it represents a much more efficient processing route, from a material perspective.

In order to study how the adsorption takes place, theoretical Langmuir and Freundlich model fits were applied to the data (see ESM, Fig. S4). The Langmuir model is based on a homogenous surface where only one molecule occupies each active site. Alternatively, the Freundlich model considers that adsorption takes place on a heterogonous surface with non-uniform distribution of adsorption energy. Based on these figures, the equilibrium data was fitted most appropriately with the Langmuir model (higher R^2 value, see Table S1) indicating that adsorption occurs as a monolayer with similar adsorption energies, which is again consitent with results found in other work on zeolites (Amanipour and Faghihian, 2017; Faghihian et al., 2015; Prajitno et al., 2020; Smičiklas et al., 2007).

The kinetics for an initial Cs^+ concentration of 5 ppm is shown in the ESM (Fig. S5) with adsorption given in terms of both relative adsorbed amount, q_t (mg/g) and percentage of initial concentration adsorbed over time. Data was fitted using the linear pseudo second order (PSO) rate model (see ESM Eq. S.3 and Fig. S6). It is observed that adsorption reaches an equilibrium plateau within 360 min (6 h) which is consistent with previous studies on similar systems (Prajitno et al., 2020). Based on Fig. S5, the R^2 of the PSO fit was 0.99, where the adsorption rate constant determined is shown in Table S2. The kinetics data is consistent to previous research on ion exchange resins, where adsorption was also fitted accurately using a PSO model (De Haro-Del Rio et al., 2015; Prajitno et al., 2020). Data also suggests that the smaller particle size of the powdered zeolite used in this study leads to fast kinetics from the PSO rate constant (k_2 equalled 0.516 g/mg.min, as given in Table S2) which is higher than natural clinoptilolite values generally found in previous research (e.g. 0.0015 (De Haro-Del Rio et al., 2015) and 0.163 g/mg.min (Prajitno et al., 2020)) and also consistent with acid activated clinoptilolite of a similar surface area (0.472 g/mg.min (Prajitno et al., 2020)). The PSO fit also indicates that the reaction is more inclined towards chemisorption at exchange sites, where the forces involved are valence forces of the same kind as those operating in the formation of chemical compounds (Ho and McKay, 1999; Liu, 2008; Smičiklas et al., 2007; Wu et al., 2009).

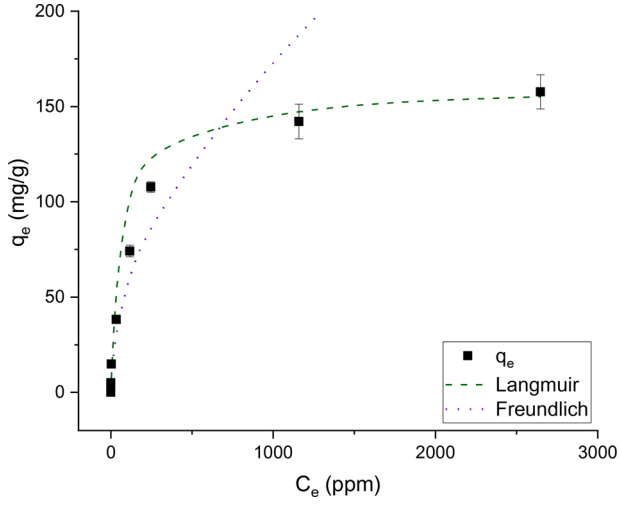

Fig. 1. Equilibrium clinoptilolite adsorption of cesium at various concentrations with Langmuir (dashed line) and Freundlich (dotted line) model fits. Error bars represent $^+$/- 1 St. Dev.

3.2. Surfactant adsorption at the solid-liquid and air-liquid surface

The particle size distributions of Cs-contaminated clinoptilolite with different surfactant concentrations of EHDa-Br and CPC, were measured to highlight any potential issues of surfactant adsorption on dispersion stability, as presented Fig. 2.

It is evident that neither surfactant causes a major shift in particle size, although both produce a small, consistent, increase as concentration is varied. The median size (d_{50}) of 5 ppm Cs^+ contaminated clinoptilolite is 8.9 μm, which increases to 10.0 μm in 20 mM EHDa-Br. Similarly, the d_{50} of Cs-contaminated clinoptilolite is 10.5 μm in 20 mM CPC surfactant. Despite the minor differences in d_{50}, there is a more significant increase in polydispersity of the systems, and an additional shoulder at larger particle sizes, which is likely associated with clinoptilolite agglomeration. As the cationic hydrophilic head group of the surfactant adsorbs onto the anionic particle surface, it should lead to the particles having greater hydrophobicity at monolayer coverage (from the hydrophobic tail group) and thus a greater surface energy in the water environment, reducing stability. While changes to particle surface energy from surfactant adsorption do not appear great enough to cause large-scale flocculation, it does not necessarily indicate that it is not sufficient for flotation. Indeed, it is known that particles can stabilise foam/froth interfaces with contact angles in the order of 60 – 70° (Hunter et al., 2008; Zhang et al., 2019a) where partially hydrophobic particles in this range are largely stable in water (Hunter et al., 2009). Therefore, large increases in size would perhaps not be expected, but the changes observed do infer substantial surfactant adsorption does occur (Azizian, 2004; Bektaş and Kara, 2004; Huang et al., 2017).

The equilibrium air-water surface tension of EHDA-Br and CPC surfactants is shown in Fig. 3, a) and b) respectively. Also given are associated Langmuir fits (using Eq. (1)) that considers monolayer adsorption of surfactant at the air-water interface to a given maximum coverage (Γ_{max}) associated with the critical micelle concentration (CMC) (Belton, 1976; Fainerman et al., 1996; James et al., 2018; Lunkenheimer et al., 2003; Stanimirova et al., 2011). The CMC for both surfactants was found experimentally to be similar, at ~0.85 mM, which is close to values reported in literature (EHDA-Br =0.8 mM and CPC = 0.84 mM) (Atkin et al., 2003). Additionally, the fitted Γ_{max} values were 3.85×10^{-6} mol/m^2 for CPC and 4.48×10^{-6} mol/m^2 EHDA-Br, and are also consistent with previous studies on CPC and other similar cationic surfactants (Ozeki et al., 1978; Phan et al., 2013). Furthermore, the R^2 values for the Langmuir fits were > 0.97 with both surfactants, giving confidence that they represented reliable models.

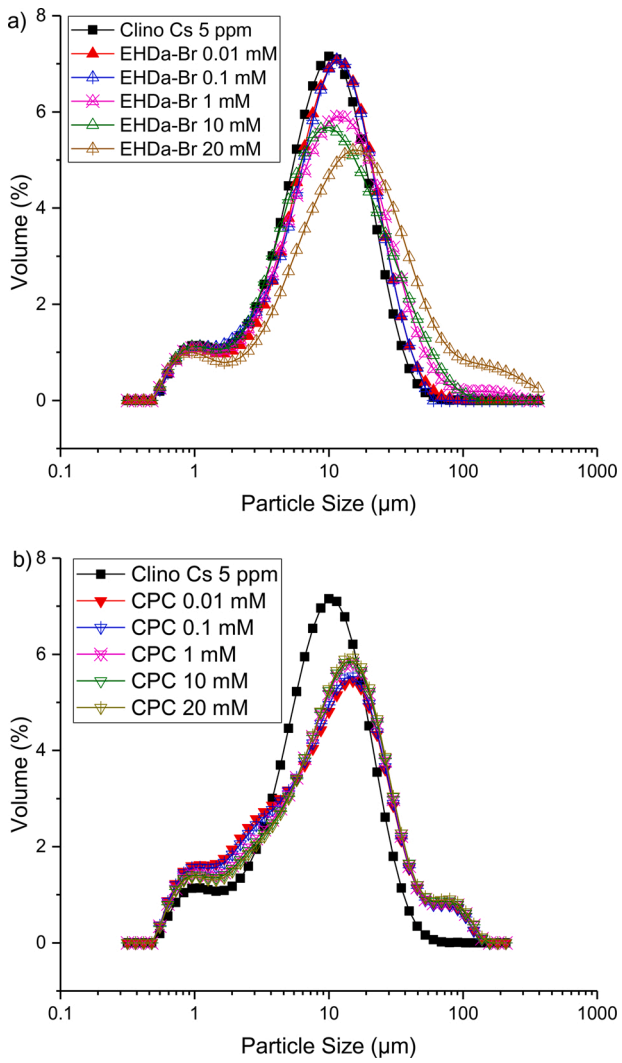

Fig. 2. Clinoptilolite particle size distribution with different surfactant concentrations of a) EHDA-Br and b) CPC.

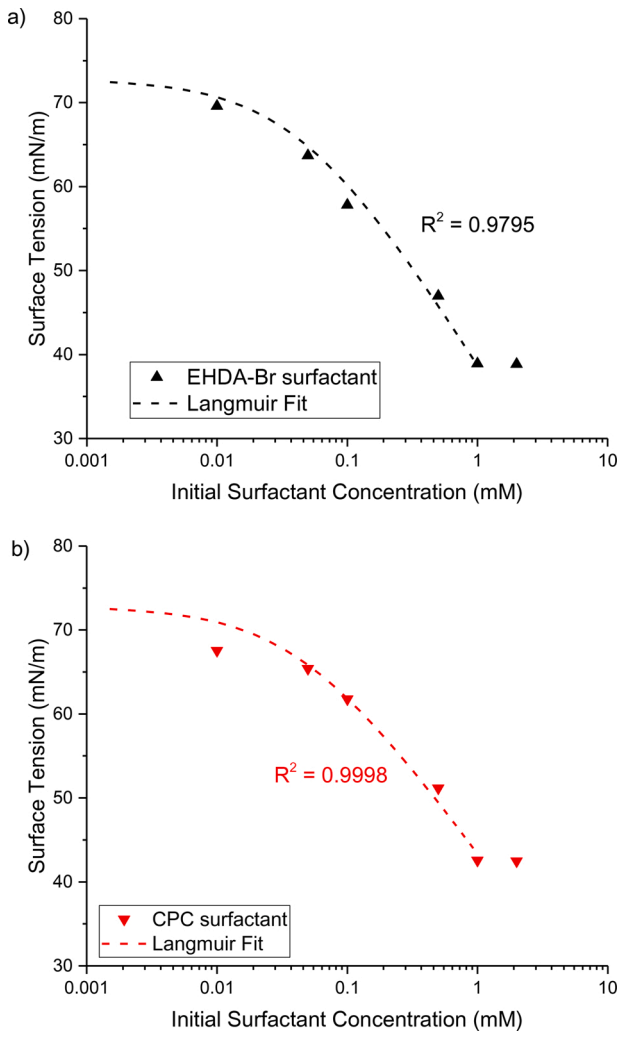

Fig. 3. Air-water surface tension versus surfactant concentration; a) EHDA-Br and b) CPC. Dashed lines represent Langmuir surfactant monolayer fits (Eq. (1)).

The surface tension of mixed surfactant-clinoptilolite systems is shown in Fig. 4, with respects to the pure surfactants, for clean clinoptilolite and material contaminated with 5 ppm Cs^+. Again, it is noted that the surface tension data for these mixtures represents that of the clear supernatants of centrifuged pre-mixed suspensions, and thus indicates the concentration of non-adsorbed surfactant remaining in the system (Abbas et al., 2020). It is evident that the surface tension of clinoptilolite mixed systems is significantly higher at low to moderate additions of either surfactant than the pure solutions, suggesting adsorption onto the clinoptilolite has substantially depleted the free-surfactant from the system, resulting in higher measured values. It also appears that the CPC performs better on Cs-contaminated clinoptilolite, as the surface tension response is almost identical to the uncontaminated system, while values for the EHDA-Br surfactant are measurably lower with cesium contamination.

Surface tension values for the mixed surfactant-clinoptilolite systems (from Fig. 4) were converted to surfactant concentration using the Langmuir fits of the pure systems (Fig. 3). Then, the amount of surfactant adsorbed was calculated from the difference to the initial concentration added. Results are presented for both EHDa-Br and CPC in Fig. 5, a) and b) respectively, in terms of the distribution of coefficient (K_d) and the percent of surfactant adsorbed (%) from natural clinoptilolite and Cs-contaminated material, based on the *equilibrium* concentrations of surfactant. These values were calculated using the ESM Eqs. S.6-S.7 (Mimura and Akiba, 1993; Mimura et al., 1991; Prajitno et al., 2020).

From Fig. 5, both natural and contaminated clinoptilolite adsorb significant amounts of either surfactant, as K_d increases by two orders of magnitude with initial surfactant concentration. At intermediate concentrations above the peak in K_d, there is a gradual reduction in the percentage for surfactant adsorbed (which is accentuated in K_d, due the relatively high solids ratio of 20 g/L). Above an equilibrium surfactant concentration of ~0.1 times the CMC, the adsorbed percent more rapidly decreases, suggesting a plateau in the adsorbed amount, although delineation between concentration regimes is not clear. It is noted that these equilibrium surfactant values are low, due to the high percentage of initial surfactant adsorbing for low to moderate concentrations.

The gradual reduction in adsorption percent above the peak K_d values is likely firstly because of increased competition for surface sites, as the number of surfactant molecules increases. It is common for small molecules and ions, that the fraction of adsorbed species will reduce with concentration, even as the total adsorbed amount increases (Prajitno et al., 2020). Indeed, the adsorption behaviour of these surfactant species is complex, due to the formation of a bilayer (or admicelle) at the solid surface (Atkin et al., 2003; Hunter et al., 2008) which produces an eventual plateau in adsorbed amount. Once a monolayer of surfactant has formed, hydrophobic interactions between monomers start increasing, leading to further adsorption occurring with the surfactant

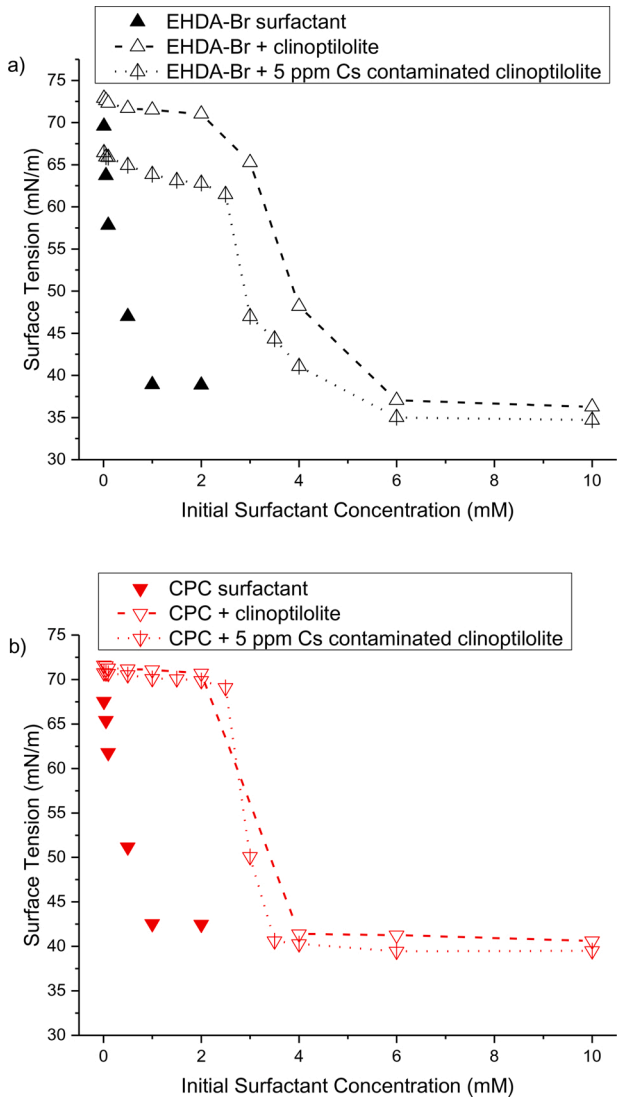

Fig. 4. Surface tension of pure EHDA-Br and CPC surfactants, as well as that of the depleted liquid after adsorption onto natural clinoptilolite and 5 ppm Cs^+ contaminated clinoptilolite, from different initial surfactant concentrations; a) EHDA-Br and b) CPC. Connecting dashed and dotted lines are to guide the eye.

head-groups facing both toward the substrate and the solution. Once the admicelle structure has fully formed (which usually occurs below the CMC) there will be no additional interaction between the surfactant and clinoptilolite, as both the surface bilayer and solution micelles will be cationic (Atkin et al., 2003; Gao et al., 1987; Hunter et al., 2008). It is also evident quantitatively that the adsorption of EHDA-Br is much more reduced with Cs-contaminated clinoptilolite, whereas very little difference is observed with CPC. It is known from ESM Fig. S1 that Cs^+ adsorption will reduce the magnitude of the surface charge, while Cs^+ ions will also occupy potential surfactant adsorption sites. As there is no significant reduction of adsorption with CPC for the same level of cesium contamination, it would suggest that the reduction in surface charge is more detrimental to EHDA-Br adsorption than CPC.

Additionally, it is important to understand whether adsorption of surfactant onto the contaminated zeolite causes some of the Cs^+ ions to be removed from exchange sites (which is possible if there is a sufficient difference in adsorption energies). Any remobilisation of Cs^+ ions may mitigate the use of surfactant enhanced flotation as a rapid separation technique. To study this effect, the amount of mobile Cs^+ was measured in the supernatants of mixed suspensions of surfactant with 5 ppm Cs-contaminated clinoptilolite (noting from ESM Fig. S5, that initial removal at this concentration is > 99 %). Fig. 6 presents these results for both surfactants, in terms of the total measured remobilised Cs^+ (in ppm) and percentage of the initial 5 ppm dose, using ESM Eq. S.7 (Prajitno et al., 2020). The amount of Cs^+ remobilised into the supernatant does increase for both surfactants up to the adsorption plateau around the CMC. Due to the stronger interaction of the CPC (shown in Fig. 5) the amount of Cs^+ ions remobilised is also correspondingly slightly greater than for EHDA-Br. However, given that the maximum removed Cs^+ was < 8 % with both surfactants, it is clear co-adsorption is energetically preferred, and such losses are not thought to be detrimental to the industrial viability of the process.

3.3. *Flotation of Cs^+ contaminated clinoptilolite*

Fig. 9 presents both the recovery and water reduction ratio for the flotation of 5 ppm Cs^+ contaminated clinoptilolite, as surfactant concentration is varied for a) EHDA-Br and b) CPC. Recovery was calculated according to ESM Eq. S.8 (Ortiz-Oliveros et al., 2012) and the water reduction ratio with Eq. (2) (Mahmoud et al., 2017). Systems with and without the addition of 50 µL MIBC frother are both included. At low concentrations of either surfactant, there is insufficient adsorption onto the contaminated clinoptilolite to enhance particle contact angles to promote a high degree of recovery. As surfactant concentrations increase to around monolayer coverage, the recovery increases in both cases. Also, both surfactants recover greater levels of contaminated clinoptilolite with the addition of frother, due to the presence of MIBC increasing the number and stability of bubbles in the froth (Albijanic et al., 2014; Le et al., 2012; Mahmoud et al., 2017). By increasing the air flowrate, the number of bubble-particle interactions is enhanced, while MIBC keeps the bubbles sufficiently stable for a required period before they detach and rupture (Darton and Sun, 1999; El-Shall et al., 2000; Hoseinian et al., 2015). Nevertheless, increasing the air flowrate further could increase turbulence levels and decrease the rupture time (Darton and Sun, 1999). It is also noted that in this system, the rupture of the bubble-particle aggregates from buoyancy driven differences is not considered significant as the particles are relatively small (George et al., 2004; Hunter et al., 2008).

The water reduction ratio data shown in Fig. 7 highlights an inverse relationship to the clinoptilolite recovery in both cases. At low surfactant concentrations, the high apparent water reduction ratio is an artefact of the low total volume of froth recovered (with therefore low associated water content). At high surfactant concentrations however, there is a clear trade-off between the recovery of clinoptilolite and the need for the froth to contain a low fraction of water to enable sufficient dewatering of the contaminated suspensions (Mahmoud et al., 2017; Rashad et al., 2019; Soliman et al., 2015).

The reason for the low water reduction ratios at high surfactant concentration is due to water entrainment in the froth. Above the CMCs, adsorption of the surfactant at the air-water interface will be maximised, creating an overly wet froth phase that will act to entrain both clinoptilolite and water, rather than separating the solid-liquid phases (Ata, 2012; George et al., 2004; Stevenson et al., 2007). In addition, above the CMC (at ~1 mM) the addition of MIBC frother does not considerably alter either contaminated clinoptilolite recovery or water reduction ratio, because of the dominating interactions of the surfactant collector on froth dynamics (Albijanic et al., 2014; Atkin et al., 2003; Polat and Erdogan, 2007; Walcarius et al., 2001; Zhang et al., 2019a). Therefore, based on Fig. 7, an optimal system was found at 0.5 mM CPC surfactant with the addition of 50 µL MIBC (Fig. 7b). For these conditions, the Cs-contaminated clinoptilolite recovery in the froth phase was ~90 %, while the water reduction ratio in the froth was still acceptable at > 4.

It is noted that dewatering ratios of 3–4 are certainly also possible in gravitational sedimentation of similar concentration dispersions, depending on the level of system aggregation (Elliott et al., 2018; Johnson et al., 2016). However, the residence time in gravitational

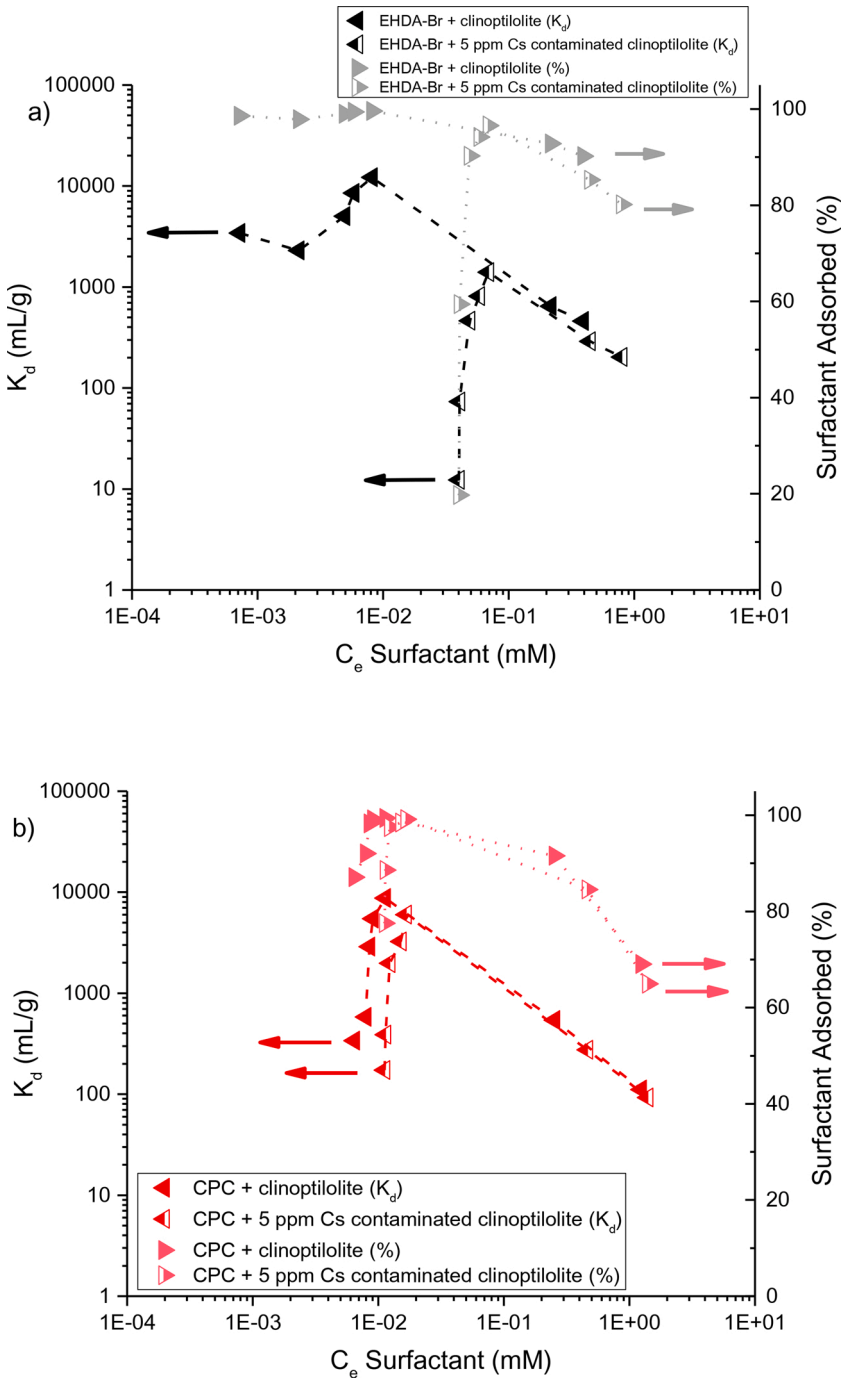

Fig. 5. Surfactant adsorption onto natural clinoptilolite and 5 ppm Cs^{+} contaminated material from different initial surfactant concentrations, shown in terms of the distribution coefficient, K_d (mL/g) (LHS) and adsorbed percent (RHS); a) EHDA-Br and b) CPC. Connecting dashed and dotted lines are to guide the eye.

thickeners for such consolidation would be tens of minutes, rather than the seconds in a flotation cell. Therefore, one of the critical benefits of flotation in this system is the rapidity of the process. Additionally, given the initial suspension concentration (of 20 g/L) a maximum possible dewatering ratio of ~ 15–20 may be expected, which would equate to a solids level of approximately 40 wt% (and so approaching or beyond the transition to a consolidated solid gel). Thus, while dewatering levels may be further optimised, ratios of ~4 are still considered relatively high. Indeed, future improvements may be gained simply by passing the concentrate froth through a second flotation cycle, which is readily achievable because of the rapid nature of flotation separation.

Using CPC surfactant at the optimum 0.5 mM concentration, the influence of varying MIBC dose was then investigated, as it has previously been demonstrated to critically alter the flotation of cesium contaminated clays (Zhang et al., 2019a). The results are shown in Fig. 8, again in terms of both clinoptilolite recovery and water reduction ratio.

Enhancement in clinoptilolite recovery is observed as MIBC dose increases towards 30 μL, whereupon it reaches a plateau for the volumes studied, indicating a limiting concentration for MIBC interaction with the froth. Considering the high surface tension data for the 5 ppm Cs-contaminated clinoptilolite with 0.5 mM CPC (Fig. 4) there is unlikely to be a large amount of unbound surfactant in this system. Thus, while it is known that surfactant mixtures may interact synergistically with

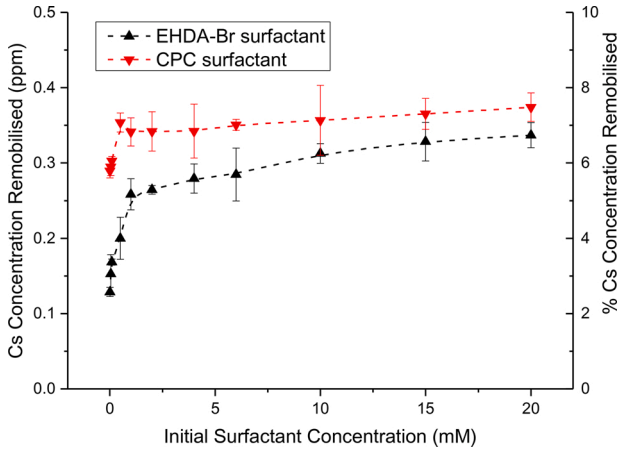

Fig. 6. The remobilised concentration of Cs^+ removed from clinoptilolite through adsorption of surfactant for different initial concentrations, shown as removed ppm from an initial 5 ppm Cs^+ solution (LHS) and percent removal (RHS). Dashed lines are to guide the eye.

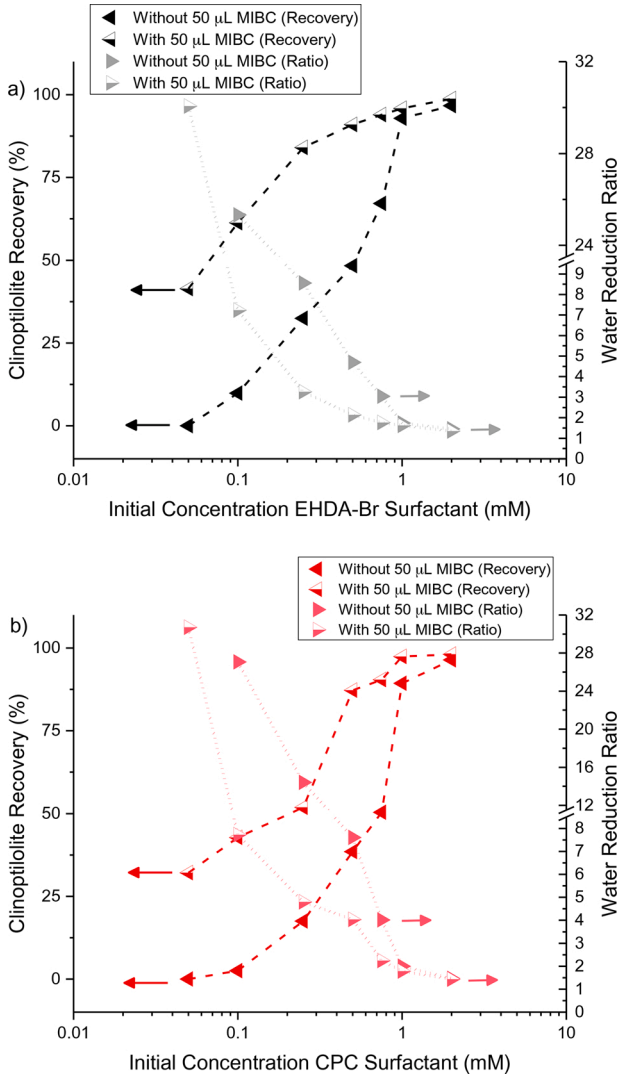

Fig. 7. The effect of MIBC frother on the flotation recovery of Cs^+ contaminated clinoptilolite (LHS) and associated water reduction ratio (RHS) with different initial surfactant concentrations; a) EHDA-Br and b) CPC. Connecting dashed lines are to guide the eye for clinoptilolite recovery and dotted lines are to guide the eye for water reduction ratio.

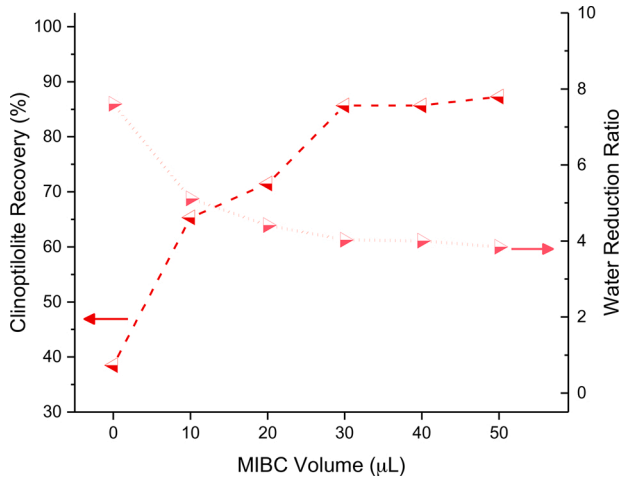

Fig. 8. The effect of different added MIBC volumes on flotation recovery of clinoptilolite (LHS) and associated water reduction ratio (RHS) with fixed 0.5 mM CPC concentration. Connecting dashed line is to guide the eye for clinoptilolite recovery and dotted line is to guide the eye for water reduction.

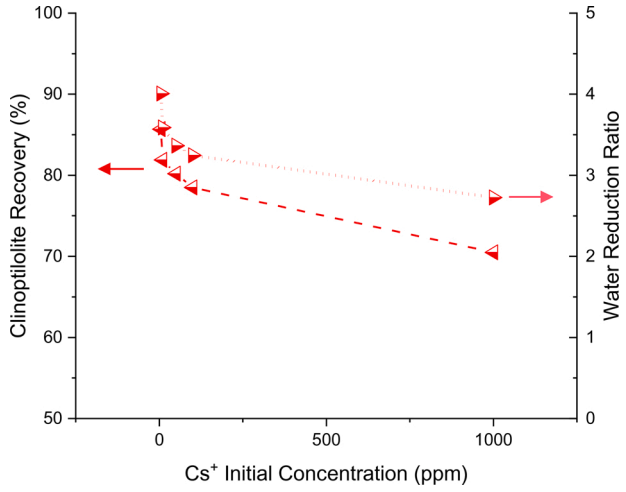

Fig. 9. The effect of different levels of adsorbed Cs^+ contamination on the flotation recovery of clinoptilolite (LHS) and associated water reduction ratio (LHS) with fixed concentration of CPC (0.5 mM) and MIBC (30 μL added).

MIBC at the air-water interface (Le et al., 2012; Phan et al., 2014; Siddiqui and Franses, 1996; Tan et al., 2005), in this case, the concentration of free CPC surfactant in solution is low (which would correspondingly explain the poor material recovery with no MIBC added). Therefore, the development of a plateau in recovery at intermediate MIBC concentrations is likely purely from the interaction mechanism of MIBC at the air-water interface, where it is known to stabilise foam films primarily through changes to interfacial elasticity rather than surface tension (Bournival et al., 2017; Tan et al., 2005). Indeed, Bournival et al. (2012) have previously demonstrated a plateau response at intermediate concentrations of MIBC in the direct coalescence of bubbles measured by high speed video, due to an increase in the dampening constant related to bubble oscillations.

Lastly, the effect of cesium contamination on clinoptilolite flotation was studied, given the potential variance in natural contamination levels (Dyer et al., 2018; Zhang et al., 2017, 2019a) and the reduction in zeta potential with cesium adsorption (ESM, Fig. S1). Here, 0.5 mM CPC surfactant and 30 μL MIBC were selected, as these parameters gave the optimum result in terms of both clinoptilolite recovery and water reduction ratio. The effect of increasing cesium contamination on

clinoptilolite during flotation is displayed in Fig. 9.

From this figure, it is clear that increasing the cesium concentration decreases both the recovery and water reduction ratio (with greatest recovery for non-contaminated material) although performance is still reasonable for cesium contamination levels < 100 ppm (which would be considered an upper limit for nuclear applications (Dyer et al., 2018)). While heavy metal ions are often added as mineral flotation activators with anionic surfactant collectors (Tian et al., 2018), in this case, both Cs^+ and the cationic CPC compete for the negative clinoptilolite surface sites (as noted in comparison to Figs. S1 and 6). It is likely that the observed decrease in flotation is due to primarily the clinoptilolite zeta potential changes (Fig. S1), where increasing the cesium concentration leads to a less negative potential. If the zeta potential becomes less negative, the adsorption of cationic surfactants to the particle surface will also correspondingly decrease. Furthermore, any reduced surfactant adsorption at the solid-liquid interface will lead to higher concentrations of free surfactant in solution and thus potentially more synergistic interactions with the MIBC increasing the foaming interactions (Polat and Erdogan, 2007; Walcarius et al., 2001). Any increase in foamability will lead to more entrainment of water in the froth, decreasing the water reduction ratio. Additionally, as the foam production is higher, the association of surfactant with contaminated clinoptilolite will be reduced, as the formation of the surfactant bilayer will occur at lower added concentrations.

Nevertheless, there are potential methods to improve the flotation of the heavily contaminated clinoptilolite that are currently being investigated. Firstly, the particle size of the powder (d_{50} of 8–10 μm) may be slightly below optimal sizes for flotation, where it is often found that particles in the range of 50–100 μm maximise recovery (Feng and Aldrich, 1999; Pérez-Garibay et al., 2014) although this range is not universal (Drzymala et al., 2020). What certainly is common is that very fine particles tend to be collected to a greater degree through entrainment in the liquid films (rather than by adsorption onto bubbles) which would lead to high recoveries, but low associated dewatering ratios, as found. Additionally, an understanding of the flotation kinetics would greatly aid in defining the most efficient column residence time for flotation using multiple passes. For the completed experiments, the flotation cell was run over 10 min, which was sufficient to achieve the maximum potential separation in a single column. Normally however, flotation kinetics follow a first order rate model, where recovery at longer times considerably reduces (Drzymala et al., 2020). This reduction is largely due to partitioning of surfactant collector and frother into the separated froth, which depletes their concentrations from the active flotation cell, reducing the foam quality and stability. Therefore, it may be more industrially effective to separate the highly contaminated systems using several flotation cells in series with low residence times.

4. Conclusions

This study examined the use of cationic surfactants to enhance the flotation of cesium contaminated powdered clinoptilolite, as an alternative to gravitational separation or the use of large resins in elution columns. Initial kinetic and equilibrium adsorption studies of cesium uptake, suggested the fine zeolite particle size (and associated large surface area to volume ratio) contributed to fast adsorption kinetics and high capacities ($q_c = 158.261$ mg/g) when compared to much previous literature on non-modified clinoptilolite (Prajitno et al., 2020). The co-adsorption of EHDa-Br and CPC surfactants onto both clean and 5 ppm Cs^+ contaminated clinoptilolite was then measured, using surface tension measurements modelled with a Langmuir isotherm. Distribution coefficients (K_d) as high as 10,000 mL/g were evident with moderate concentrations of surfactant (below those leading to bilayer formation) where CPC outperformed EHDa-Br on Cs-contaminated samples. Measurements of particle size confirmed that adsorption of surfactant monolayers did not lead to significant flocculation of the particles, suggesting good stability for flotation separation. Importantly also, less than 8 % of pre-adsorbed cesium was removed through subsequent adsorption of surfactant, highlighting that co-adsorption was energetically favourable, which is critical for flotation to be accepted as a feasible recovery technique.

In flotation tests, increasing surfactant concentration from both surfactants continually improved the recovery of 5 ppm Cs^+ contaminated clinoptilolite, while conversely impacting on performance by reducing the water reduction ratio (assumed to be due to higher levels of liquid entrainment). Moreover, the incorporation of MIBC frother considerably enhanced recovery further, for volume additions up to 30–50 μL. Overall, it was found that CPC surfactant at an 0.5 mM initial concentration and 50 μL MIBC gave optimum conditions for both recovery (at ~90 %) while maintaining an adequate water reduction ratio (~4) leading to significant dewatering and consolidation of the zeolite in the froth phase. The effect of varying initial contaminated cesium concentration on clinoptilolite was also studied, where a clear reduction in recovery was observed for levels > 80 ppm (although this concentration is well above those relevant for most nuclear applications (Borai et al., 2009)). Overall, this investigation showed that by using cationic surfactants, flotation is a viable and industrially scalable technique for the separation of fine clinoptilolite that are used for the removal of cesium ions in nuclear applications. Additionally, it may also have far reaching applications to improve the material efficiency of many types of zeolites relevant to the clean-up of industrial effluents, from sectors such as mining, textiles and consumer fine chemicals.

Data statement

The article metadata is available from the University of Leeds Research Repository: Muhammad Yusuf Prajitno, David Harbottle, Timothy Nie Hunter (2020): The effect of cationic surfactants on improving natural clinoptilolite for the flotation of cesium - Dataset University of Leeds. [Dataset]. https://doi.org/10.5518/812. Article metadata is available under a Creative Commons Attribution licence (CC-BY).

CRediT authorship contribution statement

Muhammad Yusuf Prajitno: Conceptualization, Methodology, Validation, Formal analysis, Investigation, Resources, Writing - original draft, Funding acquisition. **Suparit Tangparitkul:** Validation, Formal analysis, Investigation, Writing - review & editing. **Huagui Zhang:** Resources, Data curation, Writing - review & editing. **David Harbottle:** Supervision, Funding acquisition, Writing - review & editing. **Timothy N. Hunter:** Conceptualization, Supervision, Resources, Funding acquisition, Writing - review & editing.

Declaration of Competing Interest

We wish to confirm that there are no known conflicts of interest associated with this publication and there has been no significant financial support for this work that could have influenced its outcome, apart from the grant funding listed in the acknowledgements.

Acknowledgments

Muhammad Yusuf Prajitno was fully supported by the Indonesia Endowment Fund for Education (LPDP). TNH and DH acknowledge funding from the UK's Engineering and Physical Sciences Research Council (EPSRC) [EP/S032797/1] and the EPSRC and University of Leeds through an Impact Acceleration Account [EP/R511717/1]. HZ acknowledges the National Natural Science Foundation of China [21903015] and the Award Program of Fujian Minjiang Scholar Professorship (2018). The authors also thank the anonymous reviewers for their constructive feedback that helped improve the paper.

Appendix A. Supplementary data

Supplementary material related to this article can be found, in the online version, at doi:https://doi.org/10.1016/j.jhazmat.2020.123567.

References

Abbas, A.H., Moslemizadeh, A., Wan Sulaiman, W.R., Jaafar, M.Z., Agi, A., 2020. An insight into a di-chain surfactant adsorption onto sandstone minerals under different salinity-temperature conditions: chemical EOR applications. Chem. Eng. Res. Des. 153, 657–665.

Abusafa, A., Yücel, H., 2002. Removal of 137 Cs from aqueous solutions using different cationic forms of a natural zeolite: clinoptilolite. Sep. Purif. Technol. 28, 103–116.

Albijanic, B., Ozdemir, O., Hampton, M.A., Nguyen, P.T., Nguyen, A.V., Bradshaw, D., 2014. Fundamental aspects of bubble–particle attachment mechanism in flotation separation. Miner. Eng. 65, 187–195.

Amanipour, S., Faghihian, H., 2017. Potassium hexacyanoferrate–clinoptilolite adsorbent for removal of Cs+ and Sr2+ from aqueous solutions. Int. J. Environ. Stud. 74, 86–104.

Ames Jr., L.L., 1962. Effect of base cation on the cesium kinetics of clinoptilolite. Am. Mineral. 47, 1310–1316.

Ata, S., 2012. Phenomena in the froth phase of flotation — a review. Int. J. Miner. Process. 102-103, 1–12.

Atkin, R., Craig, V., Wanless, E.J., Biggs, S., 2003. Mechanism of cationic surfactant adsorption at the solid–aqueous interface. Adv. Colloid Interface Sci. 103, 219–304.

Aziz, M., Beheir, S.G., 1995. Removal of 60Co and 134Cs from radioactive process waste water by flotation. J. Radioanal. Nucl. Chem. 191, 53–66.

Azizian, S., 2004. Kinetic models of sorption: a theoretical analysis. J. Colloid Interface Sci. 276, 47–52.

Bektaş, N., Kara, S., 2004. Removal of lead from aqueous solutions by natural clinoptilolite: equilibrium and kinetic studies. Sep. Purif. Technol. 39, 189–200.

Belton, G.R., 1976. Langmuir adsorption, the Gibbs adsorption isotherm, and interfacial kinetics in liquid metal systems. Metall. Mater. Trans. B 7, 35–42.

Binks, B.P., 2002. Particles as surfactants—similarities and differences. Curr. Opin. Colloid Interface Sci. 7, 21–41.

Boglaienko, D., Emerson, H.P., Katsenovich, Y.P., Levitskaia, T.G., 2019. Comparative analysis of ZVI materials for reductive separation of 99Tc(VII) from aqueous waste streams. J. Hazard. Mater. 380, 120836.

Borai, E.H., Harjula, R., Malinen, L., Paajanen, A., 2009. Efficient removal of cesium from low-level radioactive liquid waste using natural and impregnated zeolite minerals. J. Hazard. Mater. 172, 416–422.

Bournival, G., Pugh, R.J., Ata, S., 2012. Examination of NaCl and MIBC as bubble coalescence inhibitor in relation to froth flotation. Miner. Eng. 25, 47–53.

Bournival, G., Ata, S., Jameson, G.J., 2017. Bubble and froth stabilizing agents in froth flotation. Miner. Process. Extr. Metall. Rev. 38, 366–387.

Charewicz, W.A., Grabowska, J., Bartsch, R.A., 2001. Flotation of Co(II), Sr(II), and Cs(I) cations with proton-ionizable lariat ethers. Sep. Sci. Technol. 36, 1479–1494.

Chorover, J., Choi, S., Amistadi, M.K., Karthikeyan, K., Crosson, G., Mueller, K.T., 2003. Linking cesium and strontium uptake to kaolinite weathering in simulated tank waste leachate. Environ. Sci. Technol. 37, 2200–2208.

Darton, R.C., Sun, K.H., 1999. The effect of surfactant on foam and froth properties. Chem. Eng. Res. Des. 77, 535–542.

De Haro-Del Rio, D.A., Al-Jubouri, S., Kontogiannis, O., Papadatos-Gigantes, D., Ajayi, O., Li, C., Holmes, S.M., 2015. The removal of caesium ions using supported clinoptilolite. J. Hazard. Mater. 289, 1–8.

Deliyanni, E.A., Kyzas, G.Z., Matis, K.A., 2017. Various flotation techniques for metal ions removal. J. Mol. Liq. 225, 260–264.

Dhenain, A., Mercier, G., Blais, J.-F., Chartier, M., 2009. Combined column and cell flotation process for the treatment of PAH contaminated hazardous wastes produced by an aluminium production plant. J. Hazard. Mater. 165, 394–407.

Ding, D., Zhang, Z., Chen, R., Cai, T., 2017. Selective removal of cesium by ammonium molybdophosphate – polyacrylonitrile bead and membrane. J. Hazard. Mater. 324, 753–761.

Drzymala, J., Bednarek-Gąbka, P., Kowalczuk, P.B., 2020. Simplified empirical and phenomenological evaluation of relation between particle size and kinetics of flotation. Powder Technol. 366, 112–118.

Dyer, A., 1993. Use of zeolites in the treatment of nuclear waste. Anal. Proc. 30, 190–191.

Dyer, A., Hriljac, J., Evans, N., Stokes, I., Rand, P., Kellet, S., Harjula, R., Moller, T., Maher, Z., Heatlie-Branson, R., 2018. The use of columns of the zeolite clinoptilolite in the remediation of aqueous nuclear waste streams. J. Radioanal. Nucl. Chem. 1–19.

Elizondo, N., Ballesteros, E., Kharisov, B., 2000. Cleaning of liquid radioactive wastes using natural zeolites. Appl. Radiat. Isot. 52, 27–30.

Elliott, L.N., Bourne, R.A., Hassanpour, A., Edwards, J.L., Sutcliffe, S., Hunter, T.N., 2018. Salt enhanced solvent relaxation and particle surface area determination via rapid spin-lattice NMR. Powder Technol. 333, 458–467.

El-Shall, H., Abdel-Khalek, N., Svoronos, S., 2000. Collector–frother interaction in column flotation of Florida phosphate. Int. J. Miner. Process. 58, 187–199.

Endo, M., Yoshikawa, E., Muramatsu, N., Takizawa, N., Kawai, T., Unuma, H., Sasaki, A., Masano, A., Takeyama, Y., Kahara, T., 2013. The removal of cesium ion with natural Itaya zeolite and the ion exchange characteristics. J. Chem. Technol. Biotechnol. 88, 1597–1602.

Faghihian, H., Marageh, M.G., Kazemian, H., 1999. The use of clinoptilolite and its sodium form for removal of radioactive cesium, and strontium from nuclear wastewater and Pb 2+, Ni 2+, Cd 2+, Ba 2+ from municipal wastewater. Appl. Radiat. Isot. 50, 655–660.

Faghihian, H., Iravani, M., Moayed, M., 2015. Application of PAN-NaY composite for CS + and SR2+ adsorption: kinetic and thermodynamic studies. Environ. Prog. Sustain. Energy 34, 999–1008.

Fainerman, V.B., Miller, R., Wüstneck, R., Makievski, A.V., 1996. Adsorption isotherm and surface tension equation for a surfactant with changing partial molar area. 1. Ideal Surface Layer. J. Phys. Chem. 100, 7669–7675.

Feng, D., Aldrich, C., 1999. Effect of particle size on flotation performance of complex sulphide ores. Miner. Eng. 12, 721–731.

Fu, F., Wang, Q., 2011. Removal of heavy metal ions from wastewaters: a review. J. Environ. Manage. 92, 407–418.

Gao, Y., Du, J., Gu, T., 1987. Hemimicelle formation of cationic surfactants at the silica gel–water interface. J. Chem. Soc. Faraday Trans. 1: Phys. Chem. Condensed Phases 83, 2671–2679.

George, P., Nguyen, A.V., Jameson, G.J., 2004. Assessment of true flotation and entrainment in the flotation of submicron particles by fine bubbles. Miner. Eng. 17, 847–853.

Han, B., Altansukh, B., Haga, K., Stevanović, Z., Jonović, R., Avramović, L., Urosević, D., Takasaki, Y., Masuda, N., Ishiyama, D., Shibayama, A., 2018. Development of copper recovery process from flotation tailings by a combined method of high–pressure leaching–solvent extraction. J. Hazard. Mater. 352, 192–203.

Han, H., Rafiq, M.K., Zhou, T., Xu, R., Mašek, O., Li, X., 2019. A critical review of clay-based composites with enhanced adsorption performance for metal and organic pollutants. J. Hazard. Mater. 369, 780–796.

Ho, Y.-S., McKay, G., 1999. Pseudo-second order model for sorption processes. Process. Biochem. 34, 451–465.

Hodges, C.S., Tangparitkul, S.M., 2019. Comment on "patterns in drying drops dictated by curvature-driven particle transport". Langmuir 35, 9988–9990.

Hoseinian, F.S., Irannajad, M., Nooshabadi, A.J., 2015. Ion flotation for removal of Ni(II) and Zn(II) ions from wastewaters. Int. J. Miner. Process. 143, 131–137.

Hu, N., Shu, T., Wu, Z., Liu, G., Li, Z., Zhao, Y., Yin, H., Huang, D., 2018. BS12-assisted flotation for the intensification of SNPs separation from CMP wastewater using a novel flotation column. J. Hazard. Mater. 344, 788–796.

Huang, Y., Takaoka, M., Takeda, N., Oshita, K., 2003. Polychlorinated biphenyls removal from weathered municipal solid waste incineration fly ash by collector-assisted column flotation. J. Hazard. Mater. 100, 259–270.

Huang, Y., Wang, W., Feng, Q., Dong, F., 2017. Preparation of magnetic clinoptilolite/CoFe2O4 composites for removal of Sr2+ from aqueous solutions: kinetic, equilibrium, and thermodynamic studies. J. Saudi Chem. Soc. 21, 58–66.

Hunter, T.N., Pugh, R.J., Franks, G.V., Jameson, G.J., 2008. The role of particles in stabilising foams and emulsions. Adv. Colloid Interface Sci. 137, 57–81.

Hunter, T.N., Wanless, E.J., Jameson, G.J., 2009. Effect of esterically bonded agents on the monolayer structure and foamability of nano-silica. Colloids Surf. A Physicochem. Eng. Asp. 334, 181–190.

James, E., Tangparitkul, S., Brooker, A., Amador, C., Graydon, A., Vaccaro, M., Cayre, O. J., Hunter, T.N., Harbottle, D., 2018. Accelerated spreading of inviscid droplets prompted by the yielding of strongly elastic interfacial films. Colloids Surf. A Physicochem. Eng. Asp. 554, 326–333.

James, A.M., Harding, S., Robshaw, T., Bramall, N., Ogden, M.D., Dawson, R., 2019. Selective environmental remediation of strontium and cesium using sulfonated hypercrosslinked polymers (SHCPs). ACS Appl. Mater. Interfaces 11, 22464–22473.

Johnson, M., Peakall, J., Fairweather, M., Biggs, S., Harbottle, D., Hunter, T.N., 2016. Characterization of multiple hindered settling regimes in aggregated mineral suspensions. Ind. Eng. Chem. Res. 55, 9983–9993.

Karimi, H., Ghaedi, M., Shokrollahi, A., Rajabi, H.R., Soylak, M., Karami, B., 2008. Development of a selective and sensitive flotation method for determination of trace amounts of cobalt, nickel, copper and iron in environmental samples. J. Hazard. Mater. 151, 26–32.

Kim, Y., Kim, Y.K., Kim, S., Harbottle, D., Lee, J.W., 2017. Nanostructured potassium copper hexacyanoferrate-cellulose hydrogel for selective and rapid cesium adsorption. Chem. Eng. J. 313, 1042–1050.

Kim, K.-W., Shon, W.-J., Oh, M.-K., Yang, D., Foster, R.I., Lee, K.-Y., 2019. Evaluation of dynamic behavior of coagulation-flocculation using hydrous ferric oxide for removal of radioactive nuclides in wastewater. Nucl. Eng. Technol. 51, 738–745.

Le, T.N., Phan, C.M., Nguyen, A.V., Ang, H.M., 2012. An unusual synergistic adsorption of MIBC and CTAB mixtures at the air–water interface. Miner. Eng. 39, 255–261.

Li, Y., Bai, P., Yan, Y., Yan, W., Shi, W., Xu, R., 2019. Removal of Zn2+, Pb2+, Cd2+, and Cu2+ from aqueous solution by synthetic clinoptilolite. Microporous Mesoporous Mater. 273, 203–211.

Liu, Y., 2008. New insights into pseudo-second-order kinetic equation for adsorption. Colloids Surf. A Physicochem. Eng. Asp. 320, 275–278.

Lunkenheimer, K., Lind, A., Jost, M., 2003. Surface tension of surfactant solutions. J. Phys. Chem. B 107, 7527–7531.

Mahmoud, M.R., Lazaridis, N.K., Matis, K.A., 2015. Study of flotation conditions for cadmium (II) removal from aqueous solutions. Process. Saf. Environ. Prot. 94, 203–211.

Mahmoud, M.R., Soliman, M.A., Rashad, G.M., 2017. Performance appraisal of foam separation technology for removal of Co(II)-EDTA complexes intercalated into in-situ formed Mg-Al layered double hydroxide from radioactive liquid waste. Chem. Eng. J. 326, 781–793.

Mavros, P., Matis, K.A., 2013. Innovations in Flotation Technology. Springer, Netherlands, Dordrecht.

Micheau, C., Schneider, A., Girard, L., Bauduin, P., 2015. Evaluation of ion separation coefficients by foam flotation using a carboxylate surfactant. Colloids Surf. A Physicochem. Eng. Asp. 470, 52–59.
Mimura, H., Akiba, K., 1993. Adsorption behavior of cesium and strontium on synthetic zeolite P. J. Nucl. Sci. Technol. 30, 436–443.
Mimura, H., Ishihara, Y., Akiba, K., 1991. Adsorption behavior of americium on zeolites. J. Nucl. Sci. Technol. 28, 144–151.
Nagasaki, S., Nakayama, S., 2015. Radioactive Waste Engineering and Management. Springer.
Ojovan, M.I., Lee, W.E., 2014. An Introduction to Nuclear Waste Immobilisation, second ed. Elsevier, Oxford.
Olatunji, M.A., Khandaker, M.U., Mahmud, H.N.M.E., Amin, Y.M., 2015. Influence of adsorption parameters on cesium uptake from aqueous solutions- a brief review. RSC Adv. 5, 71658–71683.
Ortiz-Oliveros, H.B., Flores-Espinosa, R.M., 2019. Simultaneous removal of oil, total Co and 60Co from radioactive liquid waste by dissolved air flotation. Int. J. Environ. Sci. Technol. 16, 3679–3686.
Ortiz-Oliveros, H.B., Flores-Espinosa, R.M., Jiménez-Domínguez, H., Jiménez-Moleón, M.C., Cruz-González, D., 2012. Dissolved air flotation for treating wastewater of the nuclear industry: preliminary results. J. Radioanal. Nucl. Chem. 292, 957–965.
Owens, S., Higgins-Bos, M., Bankhead, M., Austin, J., 2015. Using chemical and process modelling to design, understand and improve an effluent treatment plant. NNL Sci. 3, 1–13.
Ozeki, S., Tsunoda, M.-a., Ikeda, S., 1978. Surface tension of aqueous solutions of dodecyldimethylammonium chloride, and its adsorption on aqueous surfaces. J. Colloid Interface Sci. 64, 28–35.
Peleka, E.N., Gallios, G.P., Matis, K.A., 2018. A perspective on flotation: a review. J. Chem. Technol. Biotechnol. 93, 615–623.
Pérez-Garibay, R., Ramírez-Aguilera, N., Bouchard, J., Rubio, J., 2014. Froth flotation of sphalerite: collector concentration, gas dispersion and particle size effects. Miner. Eng. 57, 72–78.
Petrus, R., Warchoł, J., 2003. Ion exchange equilibria between clinoptilolite and aqueous solutions of Na+/Cu 2+, Na+/Cd 2+ and Na+/Pb 2+. Microporous Mesoporous Mater. 61, 137–146.
Petrus, R., Warchoł, J.K., 2005. Heavy metal removal by clinoptilolite. An equilibrium study in multi-component systems. Water Res. 39, 819–830.
Phan, C.M., Le, T.N., Nguyen, C.V., Yusa, S.-i., 2013. Modeling adsorption of cationic surfactants at air/water interface without using the gibbs equation. Langmuir 29, 4743–4749.
Phan, C.M., Nguyen, C.V., Yusa, S.-i., Yamada, N.L., 2014. Synergistic adsorption of MIBC/CTAB mixture at the air/water interface and applicability of Gibbs adsorption equation. Langmuir 30, 5790–5796.
Polat, H., Erdogan, D., 2007. Heavy metal removal from waste waters by ion flotation. J. Hazard. Mater. 148, 267–273.
Prajitno, M.Y., Harbottle, D., Hondow, N., Zhang, H., Hunter, T.N., 2020. The effect of pre-activation and milling on improving natural clinoptilolite for ion exchange of cesium and strontium. J. Environ. Chem. Eng. 8, 102991.
Rahman, R.M., Ata, S., Jameson, G.J., 2012. The effect of flotation variables on the recovery of different particle size fractions in the froth and the pulp. Int. J. Miner. Process. 106, 70–77.
Rajec, P., Domianová, K., 2007. Cesium exchange reaction on natural and modified clinoptilolite zeolites. J. Radioanal. Nucl. Chem. 275, 503–508.
Rajec, P., Macášek, F., Feder, M., Misaelides, P., Šamajová, E., 1998. Sorption of caesium and strontium on clinoptilolite-and mordenite-containing sedimentary rocks. J. Radioanal. Nucl. Chem. 229, 49–55.
Rashad, G.M., Mahmoud, M.R., Soliman, M.A., 2019. Combination of coprecipitation and foam separation processes for rapid recovery and preconcentration of cesium radionuclides from water systems. Process. Saf. Environ. Prot. 130, 163–173.
Rogers, H., Bowers, J., Gates-Anderson, D., 2012. An isotope dilution–precipitation process for removing radioactive cesium from wastewater. J. Hazard. Mater. 243, 124–129.
Shakir, K., Benyamin, K., Aziz, M., 1993. Separation of Co (II) from dilute aqueous solutions by precipitate and adsorbing colloid flotation. J. Radioanal. Nucl. Chem. 172, 329–339.
Shakir, K., Sohsah, M., Soliman, M., 2007. Removal of cesium from aqueous solutions and radioactive waste simulants by coprecipitate flotation. Sep. Purif. Technol. 54, 373–381.
Siddiqui, F.A., Franses, E.I., 1996. Surface tension and adsorption synergism for solutions of binary surfactants. Ind. Eng. Chem. Res. 35, 3223–3232.
Smičiklas, I., Dimović, S., Plećaš, I., 2007. Removal of Cs1+, Sr2+ and Co2+ from aqueous solutions by adsorption on natural clinoptilolite. Appl. Clay Sci. 35, 139–144.
Soliman, M.A., Rashad, G.M., Mahmoud, M.R., 2015. Fast and efficient cesium removal from simulated radioactive liquid waste by an isotope dilution–precipitate flotation process. Chem. Eng. J. 275, 342–350.
Stanimirova, R., Marinova, K., Tcholakova, S., Denkov, N., Stoyanov, S., Pelan, E., 2011. Surface rheology of saponin adsorption layers. Langmuir 27, 12486–12498.
Stevenson, P., Mantle, M.D., Sederman, A.J., Gladden, L.F., 2007. Quantitative measurements of liquid holdup and drainage in foam using NMRI. AIChE J. 53, 290–296.
Tan, S.N., Pugh, R.J., Fornasiero, D., Sedev, R., Ralston, J., 2005. Foaming of polypropylene glycols and glycol/MIBC mixtures. Miner. Eng. 18, 179–188.
Teh, C.Y., Budiman, P.M., Shak, K.P.Y., Wu, T.Y., 2016. Recent advancement of coagulation–flocculation and its application in wastewater treatment. Ind. Eng. Chem. Res. 55, 4363–4389.
Tian, M., Gao, Z., Sun, W., Han, H., Sun, L., Hu, Y., 2018. Activation role of lead ions in benzohydroxamic acid flotation of oxide minerals: new perspective and new practice. J. Colloid Interface Sci. 529, 150–160.
Walcarius, A., Lamdaouar, A.M., El Kacemi, K., Marouf, B., Bessiere, J., 2001. Recovery of lead-loaded zeolite particles by flotation. Langmuir 17, 2258–2264.
Wu, F.-C., Tseng, R.-L., Huang, S.-C., Juang, R.-S., 2009. Characteristics of pseudo-second-order kinetic model for liquid-phase adsorption: a mini-review. Chem. Eng. J. 151, 1–9.
Wu, H., Wang, W., Huang, Y., Han, G., Yang, S., Su, S., Sana, H., Peng, W., Cao, Y., Liu, J., 2019. Comprehensive evaluation on a prospective precipitation-flotation process for metal-ions removal from wastewater simulants. J. Hazard. Mater. 371, 592–602.
Xu, Y., Gu, P., Zhang, G., Wang, X., 2017. Investigation of coagulation as a pretreatment for microfiltration in cesium removal by copper ferrocyanide adsorption. J. Radioanal. Nucl. Chem. 313, 435–444.
Zamboulis, D., Pataroudi, S., Zouboulis, A., Matis, K., 2004. The application of sorptive flotation for the removal of metal ions. Desalination 162, 159–168.
Zhang, H., Kim, Y.K., Hunter, T.N., Brown, A.P., Lee, J.W., Harbottle, D., 2017. Organically modified clay with potassium copper hexacyanoferrate for enhanced Cs + adsorption capacity and selective recovery by flotation. J. Mater. Chem. A 5, 15130–15143.
Zhang, H., Tangparitkul, S., Hendry, B., Harper, J., Kim, Y.K., Hunter, T.N., Lee, J.W., Harbottle, D., 2019. Selective separation of cesium contaminated clays from pristine clays by flotation. Chem. Eng. J. 355, 797–804.
Zhang, M., Lu, X., Zhou, Q., Xie, L., Shen, C., 2019. Polyaluminum chloride-functionalized colloidal gas aphrons for flotation separation of nanoparticles from water. J. Hazard. Mater. 362, 196–205.